

Gravity waves over topographical bottoms: Comparison with experiment

Meng-Jie Huang, Chao-Hsien Kuo,* and Zhen Ye

Department of Physics, Wave Phenomena Lab, National Central University, Chungli, Taiwan

(Received 8 June 2004; published 11 January 2005)

The propagation of water surface waves over one-dimensional periodic and random bottoms is investigated by the transfer matrix method. For the periodic bottoms, the band structure is calculated, and the results are compared to the transmission results. When the bottoms are randomized, the Anderson localization phenomenon is observed. The theory has been applied to an existing experiment [M. Belzons *et al.*, *J. Fluid Mech.* **186**, 539 (1988)]. In general, the results are compared favorably with the experimental observation.

DOI: 10.1103/PhysRevE.71.011201

PACS number(s): 47.35.+i, 47.10.+g, 47.11.+j

I. INTRODUCTION

Propagation and scattering of gravity waves over topographical bottoms has also been and continues to be a subject of much research. A great amount of papers and monographs have been published on water waves over various topographical bottoms [1–12]. A comprehensive reference on the topic can be found in three excellent textbooks [13–15].

When multiply scattered by periodic or random topographical bottoms, the so-called band gaps and Anderson localization phenomena prevail [16,17] and have been investigated in the context of water surface waves over topographical bottoms. In 1983, Guazzelli *et al.* [18] suggested that the phenomenon of Anderson localization could be observed on shallow water waves, when the bottom has random structures. Later, Devillard *et al.* reconsidered water-wave localization inside a channel with a random bottom in a framework of the potential theory [19]. They computed the localization length for various cases. The experimental observation of water-wave localization has been subsequently suggested by Belzons *et al.* [7].

When the topographical bottoms are periodically structured, the propagation of water surface waves will be modulated accordingly. According to the Bloch theorem, waves in a periodic medium, termed Bloch waves, can be expressed in terms of the product of a plane wave and a periodic function which has the periodicity of the medium. Therefore, the waves will exhibit the properties of both plane-wave propagation and periodic modulation. Indeed, a recent experiment [20] has used gravity waves to illustrate the phenomenon of Bloch waves over a two-dimensional periodic bottom. This pioneering experiment has made it possible that the abstract concept be presented in an unprecedentedly clear manner. The experimental results have also been matched by a theoretical analysis in Ref. [21].

Motivated by these developments, we wish to further consider the propagation and localization properties of water surface waves. Two-dimensional situations have been considered elsewhere [22]. There the propagation of water waves over cylindrical steps has been considered. It is shown that the waves can be localized spatially through the process of multiple scattering and wave interference. When local-

ized, the transmission of the waves falls off exponentially in all directions, and a cooperative behavior appears.

In this paper, we will consider water waves over one-dimensional uneven bottoms. The systems adopted here are from the experiment of Belzons *et al.* [7]. We present a theoretical analysis of the previous experimental results [7]. The formulation in Ref. [23] will be used for this purpose. Comparison between the experimental and theoretical results, in return, provides a verification of the theory. We will study the band structure of periodic cases, the effect of randomness on wave propagation, the relation between the band gaps and localization, and the amplitude or energy distribution over the structured bottoms. The dependence on parameters, such as the frequency, water depth, and variations of the height and width of the obstacle steps, will be examined in detail. Although the experiment to be analyzed here was done nearly 20 years ago, to the best of our knowledge, however, there have been no further experiments which have been done on water waves in the context of localization effects. Even existing limited experimental results have not been thoroughly analyzed. The present paper bridges the gaps with the hope that further experimental investigations may be arranged. From the results, we can see a few differences between two-dimensional (2D) and one-dimensional (1D) cases. For example, in 2D, localized waves start the exponential decay right from the transmission site, while in 1D, the exponential decay starts when waves have traveled a reasonably long distance. We also emphasize that the present paper has been limited to consider linear water waves. For nonlinear wave situations, readers may refer to Ref. [12].

The paper will be constructed as follows. In the next section, we will present the formulation and parametrization of the problem. The results and discussion will be presented in Sec. III, followed by a summary in Sec. IV.

II. GENERAL FORMULATION

A theory of water-wave propagation over step-mounted bottoms has been recently proposed and developed in Refs. [21,23]. This formulation has been used earlier in interpreting some experimental data [21]. While the details can be referred to in Ref. [23], here we only present the final equation. After the Fourier transformation, the equation describing the wave of frequency ω over topographical bottoms is

*Electronic address: chkuo@phy.ncu.edu.tw

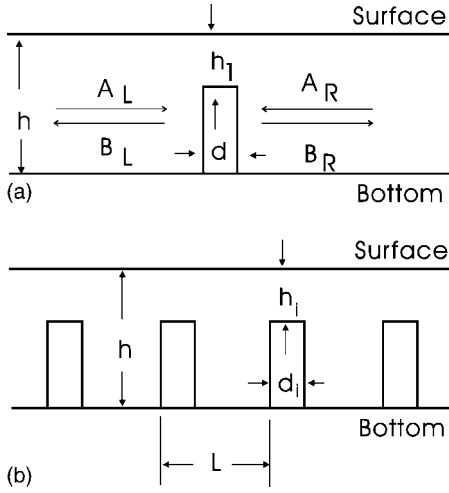


FIG. 1. Conceptual layouts.

$$\nabla \left(\frac{1}{k^2} \nabla \eta \right) + \eta = 0, \quad (1)$$

where k satisfies

$$\omega^2 = gk(\vec{r}) \tanh[k(\vec{r})h(\vec{r})], \quad (2)$$

where η is the surface displacement, g is the gravity acceleration constant, and h is the depth from the surface. For a fixed frequency, the variation of the wave number k with the topographical bottom is determined by the depth function h .

From Eq. (1), we have the conditions linking domains with different depths as follows: both η and

$$\frac{\tanh(kh)}{k} \eta = \frac{\omega^2}{gk^2} \eta$$

are continuous across the boundary.

A. Application to one-dimensional situations

1. Single step

First, consider a step with width d and a wave propagating along the x direction. The conceptual layout is as in Fig. 1(a). We use the standard transfer matrix method to solve for the wave transmission across the step.

The waves on the left, within, and on the right side of the step can be generally rewritten as

$$\begin{aligned} \eta_L &= A_L e^{ik_L x} + B_L e^{-ik_L x}, \\ \eta_M &= A_M e^{ik_M x} + B_M e^{-ik_M x}, \\ \eta_R &= A_R e^{ik_R x} + B_R e^{-ik_R x}. \end{aligned} \quad (3)$$

The subscripts L , M , and R represent the quantities on the left side, in the middle, and on the right side of the step, respectively.

The boundary conditions lead to the following equations:

$$A_L e^{ik_L x_L} + B_L e^{-ik_L x_L} = A_M e^{ik_M x_L} + B_M e^{-ik_M x_L}, \quad (4)$$

$$\frac{1}{k_L} (A_L e^{ik_L x_L} - B_L e^{-ik_L x_L}) = \frac{1}{k_M} (A_M e^{ik_M x_L} - B_M e^{-ik_M x_L}) \quad (5)$$

and

$$A_M e^{ik_M x_R} + B_M e^{-ik_M x_R} = A_R e^{ik_R x_R} + B_R e^{-ik_R x_R}, \quad (6)$$

$$\frac{1}{k_M} (A_M e^{ik_M x_R} - B_M e^{-ik_M x_R}) = \frac{1}{k_R} (A_R e^{ik_R x_R} - B_R e^{-ik_R x_R}). \quad (7)$$

In these equations, $x_{L,R}$ stands for locations of the left and right sides of the step, respectively, and $x_R - x_L = d$.

The first set of boundary equations gives the matrix relation

$$\begin{pmatrix} A_L \\ B_L \end{pmatrix} = T_{LM} \begin{pmatrix} A_M \\ B_M \end{pmatrix}, \quad (8)$$

with

$$T_{LM} = \frac{1}{2} \begin{pmatrix} (1 + g_{LM}) e^{i(k_M - k_L)x_L} & (1 - g_{LM}) e^{-i(k_M + k_L)x_L} \\ (1 - g_{LM}) e^{i(k_M + k_L)x_L} & (1 + g_{LM}) e^{-i(k_M - k_L)x_L} \end{pmatrix} \quad (9)$$

and

$$g_{LM} = \frac{k_L}{k_M}.$$

Similarly, we can derive

$$\begin{pmatrix} A_M \\ B_M \end{pmatrix} = T_{MR} \begin{pmatrix} A_R \\ B_R \end{pmatrix}, \quad (10)$$

with

$$T_{MR} = \frac{1}{2} \begin{pmatrix} (1 + g_{MR}) e^{i(k_R - k_M)x_R} & (1 - g_{MR}) e^{-i(k_R + k_M)x_R} \\ (1 - g_{MR}) e^{i(k_R + k_M)x_R} & (1 + g_{MR}) e^{-i(k_R - k_M)x_R} \end{pmatrix} \quad (11)$$

and

$$g_{MR} = \frac{k_M}{k_R}.$$

From Eqs. (9) and (11), we obtain the following solution in the transfer matrix form:

$$\begin{pmatrix} A_L \\ B_L \end{pmatrix} = T_{LR} \begin{pmatrix} A_R \\ B_R \end{pmatrix}, \quad (12)$$

with

$$T_{LR} = T_{LM} T_{MR}. \quad (13)$$

Equation (12) relates the waves on the left to the right side of the step.

2. Case of N steps

Now we consider N steps in a uniform medium of wave number k . The illustration is in Fig. 1(b). The step widths are d_i and the water depths over the steps are h_i . The wave number over the step is denoted by $k_i (i=1, \dots, N)$. They satisfy the following relations, respectively:

$$\omega^2 = gh \tanh(kh), \quad \omega^2 = gh_i \tanh(k_i h_i). \quad (14)$$

Clearly, the coefficients on the leftmost region is related to the most-right-hand region by

$$\begin{pmatrix} A_L \\ B_L \end{pmatrix} = T(N) \begin{pmatrix} A_R \\ B_R \end{pmatrix}, \quad (15)$$

with

$$T(N) = \prod_{i=1}^N T_i. \quad (16)$$

The matrix T_i is the transfer matrix for the i th step and will be given below.

Let us consider a unit plane-wave propagation along the x direction, and explore the reflection and transmission properties. In this case, clearly we have

$$A_L = 1, \quad B_R = 0. \quad (17)$$

$B_R=0$ is the common radiation condition. Thus from Eq. (15) we arrive at the solutions

$$A_R(N) = \frac{1}{T_{11}(N)}, \quad B_L(N) = \frac{T_{21}(N)}{T_{11}(N)}. \quad (18)$$

The subscripts denote the corresponding matrix elements.

The transmission and reflection coefficients are defined as

$$T = |A_R(N)|^2, \quad R = 1 - T. \quad (19)$$

Now we construct the T matrix for each step. In the current case, we have

$$g_{LM}(i) = \frac{k}{k_i}, \quad g_{MR}(i) = \frac{k_i}{k} \quad (20)$$

and

$$k_L = k, \quad k_M = k_i, \quad k_R = k. \quad (21)$$

We denote $g_{s,i} = k/k_i$. Therefore,

$$T(i) = \frac{1}{4} \begin{pmatrix} (1 + g_{s,i})e^{i(k_i L - kL)x_{i,L}/L} & (1 - g_{s,i})e^{-i(k_i L + kL)x_{i,L}/L} \\ (1 - g_{s,i})e^{i(kL + k_i L)x_{i,L}/L} & (1 + g_{s,i})e^{-i(k_i L - kL)x_{i,L}/L} \end{pmatrix} \times \begin{pmatrix} \left(1 + \frac{1}{g_{s,i}}\right)e^{i(kL - k_i L)(x_{i,L} + d_i)/L} & \left(1 - \frac{1}{g_{s,i}}\right)e^{-i(kL + k_i L)(x_{i,L} + d_i)/L} \\ \left(1 - \frac{1}{g_{s,i}}\right)e^{i(kL + k_i L)(x_{i,L} + d_i)/L} & \left(1 + \frac{1}{g_{s,i}}\right)e^{-i(kL - k_i L)(x_{i,L} + d_i)/L} \end{pmatrix}, \quad (22)$$

where $x_{i,L}$ is the coordinate of the left side of the i th step.

2. Band structure for periodic cases

For the periodically arranged steps with $d_i = d$ and $h_i = h_1$, the band structure can be solved. According to Bloch theo-

$$T_i = \frac{1}{4} \begin{pmatrix} (1 + g_{s,i})e^{i(k_i - k)x_{i,L}} & (1 - g_{s,i})e^{-i(k_i + k)x_{i,L}} \\ (1 - g_{s,i})e^{i(k + k_i)x_{i,L}} & (1 + g_{s,i})e^{-i(k_i - k)x_{i,L}} \end{pmatrix} \times \begin{pmatrix} (1 + 1/g_{s,i})e^{i(k - k_i)x_{i,R}} & (1 - 1/g_{s,i})e^{-i(k + k_i)x_{i,R}} \\ (1 - 1/g_{s,i})e^{i(k + k_i)x_{i,R}} & (1 + 1/g_{s,i})e^{-i(k - k_i)x_{i,R}} \end{pmatrix}. \quad (22)$$

B. Simulation setup

1. Nondimensional parametrization

Consider an infinite periodic array of the steps, as shown in Fig. 1. The lattice constant is L . For random arrays, L refers to the average distance between two adjacent steps.

The dispersion relation is

$$\omega^2 = gk \tanh(kh).$$

This can be rewritten as

$$\frac{\omega^2}{\omega_0^2} = (kL) \tanh\left((kL) \frac{h}{L}\right),$$

with

$$\omega_0^2 = \frac{g}{L}.$$

Therefore, in all later computations, the length can be scaled by L , the frequency by ω_0 , and the wave number by kL .

The wave numbers in the medium and within the steps are given by (at the same frequency)

$$\frac{\omega^2}{\omega_0^2} = (kL) \tanh\left((kL) \frac{h}{L}\right), \quad (23)$$

$$\frac{\omega^2}{\omega_0^2} = (k_i L) \tanh\left((k_i L) \frac{h_i}{L}\right). \quad (24)$$

This leads to

$$g_{s,i} = \frac{kL}{k_i L},$$

and the transfer matrix of the i th step is

rem, the water surface displacement η can be expressed as

$$\eta(x) = \xi(x)e^{iKx}, \quad (26)$$

where K is the Bloch wave number and $\xi(x)$ is a periodic function modulated by the periodicity of the structure—i.e.,

$\xi(x+L)=\xi(x)$. The relation between K and the frequency ω can be obtained by taking Eq. (26) into Eq. (15).

We can derive an equation determining the band structure in the periodic case,

$$\begin{aligned} \cos(KL) = & \cos[k_1L(d/L)]\cos[kL(L-d)/L] \\ & - \cosh(2\xi)\sin[k_1L(d/L)]\sin[kL(L-d)/L], \end{aligned} \quad (27)$$

where

$$\xi = \ln(q), \quad \text{with } \omega^2 = gk_1 \tanh(kh_1), \quad q^2 = \frac{k_1}{k}.$$

3. Random situations

There are a number of ways to introduce the randomness. (1) Variation in the height of the steps: with the fixed widths and positions of the steps, the height of the steps can be varied in a controlled way. For example, the height of the steps can be varied randomly between $[H_0 - \Delta H, H_0 + \Delta H]$. (2) Positional disorders: initially, the steps are arranged in a lattice form. Then allow each step to move randomly around its initial position. The allowing range for movement can be controlled and denotes the level of randomness. The extreme case is completely randomness. (3) Width randomness: we can also introduce the randomness for the widths of the steps. In the simulation, we will consider the randomness introduced in the experiment [7].

When randomness is introduced, a few definitions are in order. The most important quantity is the Lyapounov exponent γ . Its definition is

$$\gamma = \lim_{N \rightarrow \infty} \langle \gamma_N \rangle, \quad (28)$$

where

$$\gamma_N \equiv -\frac{1}{N} \ln[|A_R(N)|].$$

Here $|A_R(N)|^2$ is the transmission coefficient for a system with N random steps, referring to Eq. (18),

$$|A_R(N)|^2 = \frac{1}{|T_{11}(N)|^2}.$$

The symbol $\langle \cdot \rangle$ denotes the average over the random configuration. The inverse of the Lyapounov exponent characterizes the localization length—i.e., $\xi = \gamma_N^{-1}$.

III. RESULTS AND DISCUSSION

The systems are from the previous experiment [7]. That is, the bottoms are mounted with a series of steps and these steps are either regularly or randomly but on average regularly placed on the bottoms. Three cases are considered and are illustrated by Fig. 2. In the bed P case, the averaged water depth is H_0 , the periodicity is $2L_0$, and the step variation is fixed at σH . In the bed RS case, the averaged water depth is H_0 , the step variation is fixed at σH , and the separation between steps is uniformly distributed with $[d_0 - \Delta d, d_0 + \Delta d]$. In the bed R case, both the height and separation between the

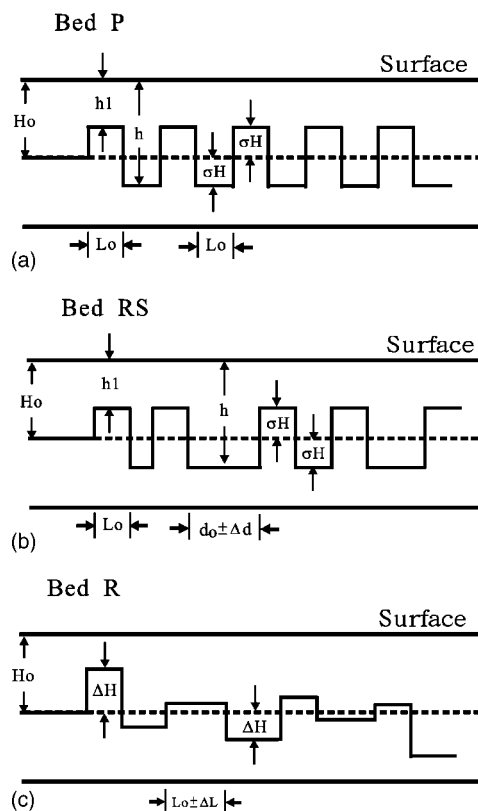


FIG. 2. Situations considered in this paper, adopted from Fig. 2 of Ref. [7]. (a) Bed P case: in this case, the steps are mounted periodically with lattice constant $2L_0$; the variation of the steps σH is fixed. (b) Bed RS case: in the case, the steps are allowed to move randomly from their initial periodic positions, as set in the bed P case—the allowed range is denoted as $\pm \Delta L$ and the variation of the steps σH is fixed. (c) Bed R: in this case, both the heights and the widths are allowed to vary randomly from their initial values in the bed P case within the ranges $[H_0 - \Delta H, H_0 + \Delta H]$ and $[L_0 - \Delta L, L_0 + \Delta L]$.

steps are allowed to vary randomly, but within the ranges $[H_0 - \Delta H, H_0 + \Delta H]$ and $[L_0 - \Delta L, L_0 + \Delta L]$, respectively.

The experimental setups have been described in Sec. II of Ref. [7]. We briefly repeat here. The experiments were carried out in a glass-walled wave tank with length 4 m and width 0.39 m. A bottom composed of periodic or random steps was built into a flat bottom with mean water depth H_0 . The different bottoms varied only along the tank so that, apart from weak edge effects, the propagation of waves is considered to be one dimensional. The resolution of the water depth is estimated at about 0.2 mm.

A. Band structure and transmission

First, we consider the first case in the experiment: the periodic case—i.e., the bed P case. For this case, the band structure and the transmission are computed for two water depths. In both cases, the width of the steps is $L_0 = 4.1$ cm; therefore, the periodicity is 8.2 cm. The results are shown in Fig. 3. From the band structure results in (a1) and (b1), we observe that for the small water depth ($H_0 = 1.75$ cm), there

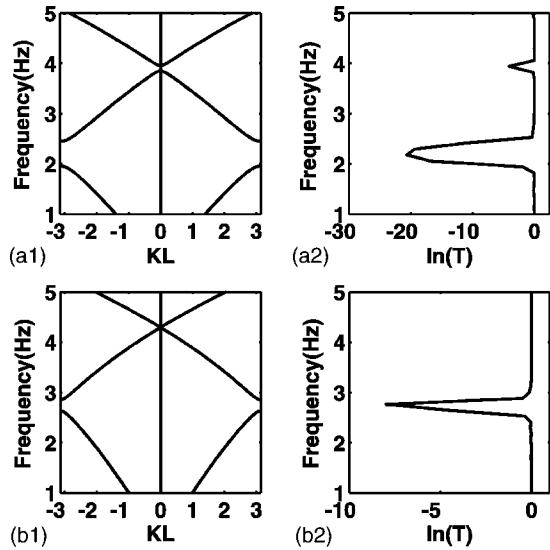


FIG. 3. Band structure and transmission for the bed P case in two situations, referring to Fig. 2(a): (a1) and (a2) The average water depth is $H_0=1.75$ cm, and the height variation is $\sigma H/H_0=0.43$. (b1) and (b2) The average water depth is $H_0=3$ cm, and the height variation is $\sigma H/H_0=0.25$. The left and right panes show the band structure and transmission results, respectively. The transmission is presented in the logarithmic scale for 100 steps.

are two band gaps in the frequency range measured in the experiment, while in the deeper case ($H_0=3$ cm) there is one band gap. The locations of the band gaps match the inhibited transmission regimes. The width of the gap and the inhibition effect tend to decrease with frequency as shown by (a1) and (a2). This is understandable. In the high-frequency limit—i.e., when $kh \gg 1$ —the dispersion relation in Eq. (2) approaches $\omega^2=gk$. Therefore the importance of the bottom structure will decrease with increasing frequency. The results in Fig. 3 will help us comprehend the later results.

B. Reflection coefficient

In the experiment [7], the reflection coefficients are measured for the three cases: bed P, bed R, and bed RS cases. Two average water depths are considered: $H_0=1.75$ and 3 cm. We have considered all the cases and applied the formulation in Sec. II to obtain corresponding results. In Fig. 4, we present our theoretical results. For the convenience of the reader and as a comparison, we also replot the experimental results in the same figure (left panel). We have taken into account two random configuration numbers in the simulation: one is 5 random configurations—i.e., the middle panel—which is taken as the same as in the experiment; the other in the right panel is more than 10 000 random configurations to ensure the stability of the averaging results. All the parameters are repeated from Ref. [7].

Figures 4(a1), 4(a2), and 4(a3) compare the results for the bed RS and bed P cases with averaged water depth $H_0=1.75$ cm and step width $L_0=4.1$ cm. For both cases, the ratio $\sigma H/H_0$ is fixed at 0.43; i.e., there is no variation in the step heights. In the bed RS case, the disorder is introduced to the separation between steps; that is, the separation is ran-

domly chosen with uniform distribution within $[2 \text{ cm}, 8 \text{ cm}]$ or $[d_0-3, d_0+3]$ with $d_0=5$ cm. In the simulation, the total number of steps is 58. We have taken two numbers of random configuration in the simulation. One is 5 (a2), which complies with the experiment, and the other (a3) is 10 000 times, so to ensure the stability of the averaging. The experimental data are shown in (a1). The comparison of (a1), (a2), and (a3) indicates the following. Overall speaking, the theoretical results capture well the qualitative features observed experimentally and agree to a certain extent with the experimental results.

First we consider the bed P case. (1) The theoretically predicted positions of the reflection peaks agree well with the experimental observation in the bed P case. These positions also coincide with the band gaps from the band structure computation in Fig. 1. (2) In the bed P case, the reflection coefficient reaches its maximum value of 1 within the band gaps as expected, while the experimental values are always smaller than 1 for the frequency range considered. A possible reason for this discrepancy may be that in the theoretical simulation, we did not take into account possible dissipation effects caused by such as viscosity and thermal exchange; some of these effects have been discussed in Ref. [7]. These effects tend to prevent waves from propagation. (3) The theoretical width of the first reflection peak in the bed P case matches well that observed, but the theoretical width of the second reflection peak at about 4 Hz is narrower than that from the experiment. In fact, the experimentally measured widths of the two reflection peaks are more or less the same. Since the effects of the periodic bottom diminish with increasing frequency as discussed above, we may conclude that there are other effects which could broaden the reflection peak at 4 Hz, and these effects may include those from the dissipation, nonlinearity, and evanescent mode leakage. These effects have not been considered in the current theory [23].

Now we consider the bed RS case. (1) Again, except for the peak values in the reflection, the theoretical results reproduce the experimental observation reasonably well in general, particularly at the strong reflection located at about 2 Hz. (2) Different from the bed P case, the width of the first reflection peak at 2 Hz is wider in theory than in the experiment. (3) In both theory and experiment, a second reflection peak is noticed within 4 and 5 Hz. (4) An obvious difference between the theory and experiment is at low frequency around 1.2 Hz, a strong sharp reflection peak appears at 1.2 Hz in the experiment, but is absent in the theory. This experimental observation differs from previous observations in acoustic or optical systems [17]. In acoustic or optical systems, the disorder effect decreases as the frequency decreases. Therefore, waves tend to diffuse away, leading to weaker reflections at low frequencies. In fact, the result of the reflection measurement is also in disagreement with the localization measurement shown in Fig. 15 of Ref. [7] where it is shown that the localization length at 1.2 Hz is even longer than at 1.5 Hz at which the reflection is small; the longer the localization length, the weaker the reflection. (5) Increasing the number of random configuration tends to smooth the curves.

The comparison between the theoretical and experimental reflection results for the bed P and bed R cases with H_0

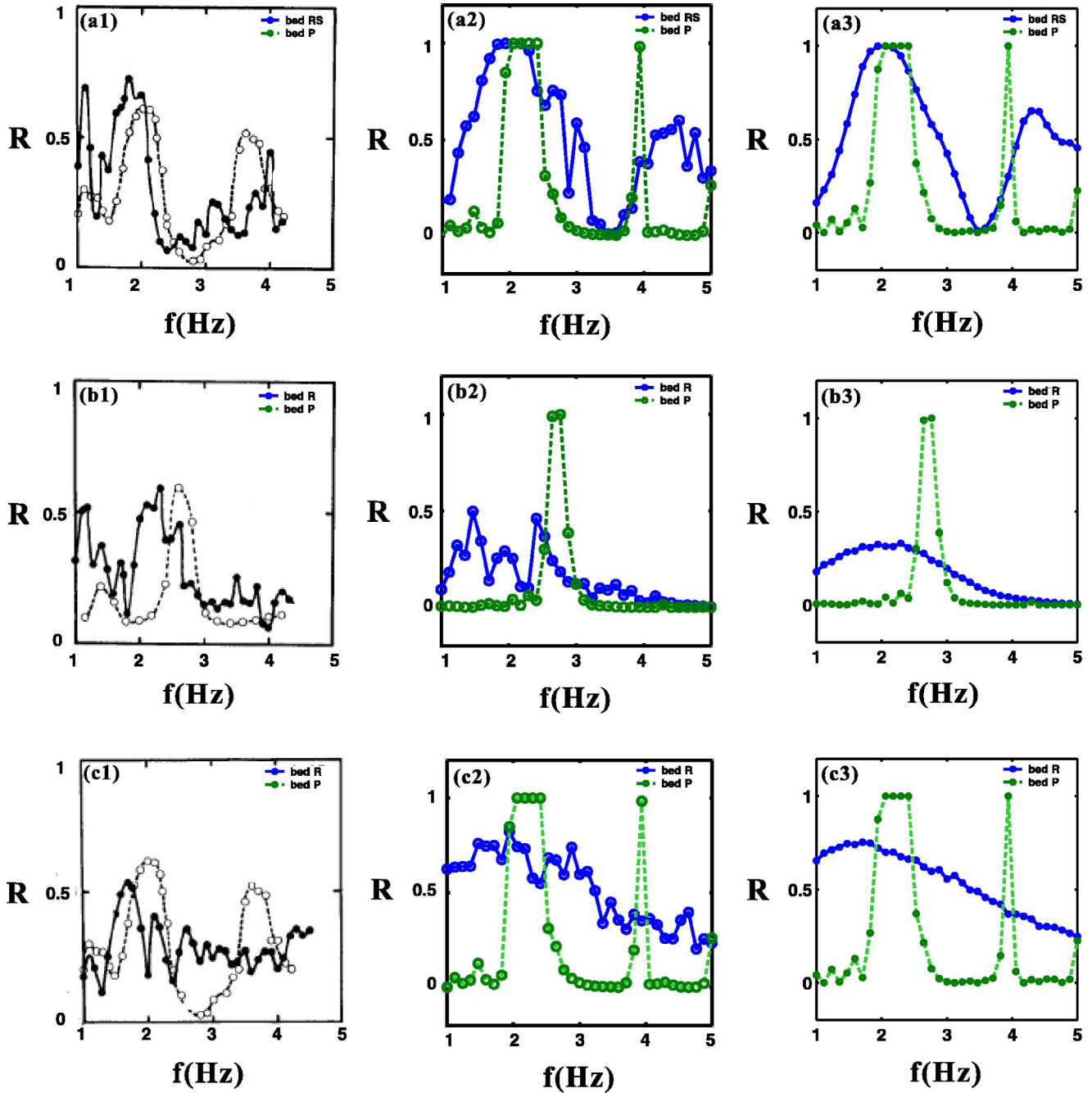


FIG. 4. Reflection versus frequency for the bed RS and P cases with three average water depths. Left panel: the results from the experiment [7]. Middle panel: the theoretical results with the average over five random configurations. Right panel: the theoretical results with the average over 10 000 random configurations, so to make sure the stability of the average.

=3 cm is shown by Figs. 4(b1), 4(b2), and 4(b3). The parameters are as follows. (1) Bed P: $\sigma H/H_0=0.25$, $L_0=4.1$ cm; (2) Bed R: the separation between steps varies completely randomly within $L_0 \pm \Delta L$ with $\Delta L=2$ cm, and the height of the steps varies uniformly within $H_0 \pm \Delta H$ with $\Delta H=1.26$ cm. The number of steps is 58. In (b2), five random configurations are used for averaging, and in (b3) 10 000 random configurations are used to ensure the stability of the averaging. In the bed P case, except at the reflection peak, the theoretical results reproduce very well the experimental observation. In the bed R case, the theoretical results

also match that from the experiment in both the qualitative structure and the magnitude, referring to (b1) and (b2). The existing deviation may result from an insufficient random average.

The comparison between the theoretical and experimental reflection results for the bed P and bed R cases with $H_0=1.75$ cm is shown by Figs. 4(c1), 4(c2), and 4(c3). The parameters are as follows. (1) Bed P: $\sigma H/H_0=0.43$, $L_0=4.1$ cm. (2) Bed R: the separation between steps varies completely randomly within $L_0 \pm \Delta L$ with $\Delta L=2$ cm, and the height of the steps varies uniformly within $H_0 \pm \Delta H$ with

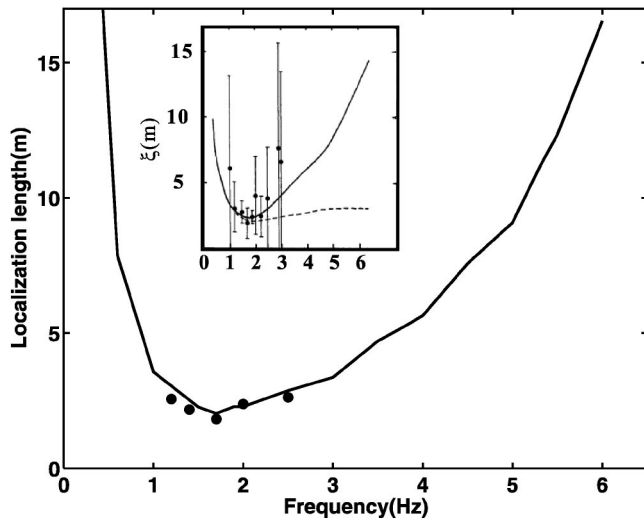


FIG. 5. Localization length versus frequency for the bed R case. The experimental results are shown in the inset, and the legends can be referred to in [7]; for example, the lines in the inset refer to the results from two other theoretical calculation [7]. The five black dots denote the results from an averaging over five random configurations.

$\Delta H=1.24$ cm. The number of steps is 58. In (c2), five random configurations are used for averaging, and in (c3) 10 000 random configurations are used to ensure the stability of the averaging. The bed P case has been discussed in the above. In the bed R case, the general features of the experimental and theoretical results seem to be agreeable with each other. The predicted reflection curve starts to match qualitatively the experimental data from about 3 Hz. The discrepancy at low frequencies is, again, noticeable.

C. Localization length

In the experiment [7], the localization length is extracted from the measurement of the total wave amplitude attenua-

tions. In the simulation, the localization length is obtained from the inverse of the Lyapounov exponent given in Eq. (28). Here the bed R case is considered and the parameters are $H_0=1.75$ cm, $L_0=4.1$ cm, and the height of the steps and the separation between steps vary randomly within the ranges $[H_0-\Delta H, H_0+\Delta H]$ and $[L_0-\Delta L, L_0+\Delta L]$ respectively; here, $\Delta H=1.2425$ cm and $\Delta L=2$ cm. Ten thousand steps and 10 000 random configurations have been used in the simulation to ensure the stability of the numerical results.

The numerical and experimental results are shown in Fig. 5. Here the localization length is plotted against the frequency. The results from Ref. [7] are shown in the inset. A few observations are in order. (1) In Ref. [7], the authors have used a potential formulation to obtain the localization length, denoted by the solid length in the inset. By eye inspection, we see that the present numerical results agree remarkably well with the results from the potential theory, thus providing further support for the present relatively simple theory, stemming from Ref. [23]. (2) The numerical results also agree with the averaged experimental data in the vicinity of the frequency 2 Hz. (3) There is a huge fluctuation in the experiment results. From our simulation, we think that such a significant deviation is due to insufficient average numbers, an obvious limitation on any experiment. This is particularly an important factor when the localization length is long. Nevertheless, the agreement shown in Fig. 5 is encouraging.

D. Behavior of the wave amplitude along the random bed

In the experiment, the variation of the wave amplitude along the random bed is also measured. Both bed RS and bed R cases are considered. The parameters used in the experiment [7] are summarized as follows. In the bed RS case, $H_0=1.75$ cm, $\sigma H/H=0.43$, $L_0=4.1$ cm, and the separation between steps varies randomly in the range of [2 cm, 8 cm]. In the bed R case, $H_0=1.75$ cm, $L_0=4.1$ cm, and the height of the steps and the separation between steps vary randomly

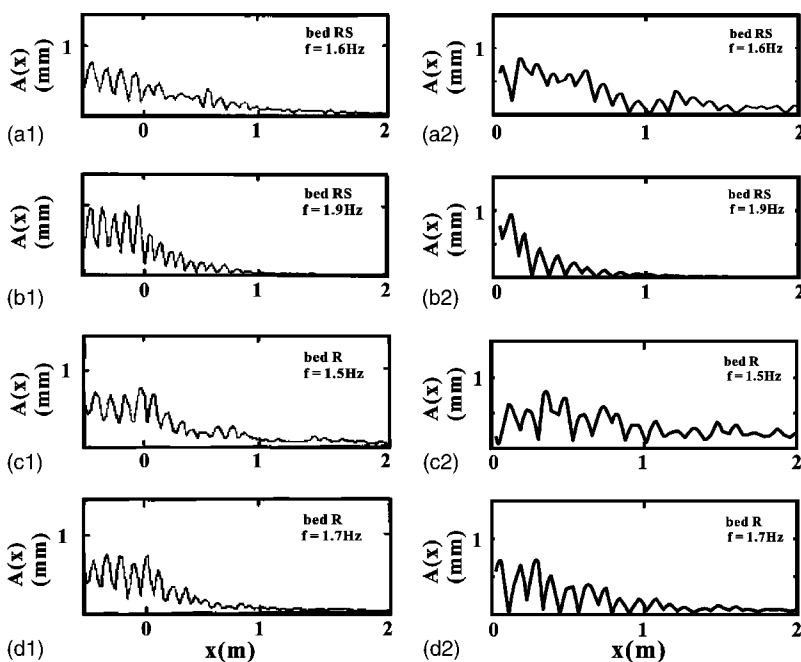


FIG. 6. Variation of the amplitude of wave elevation along the wave tank for the bed RS and bed R cases for different frequencies. The experimental [7] and numerical results are shown in the left and right panels, respectively.

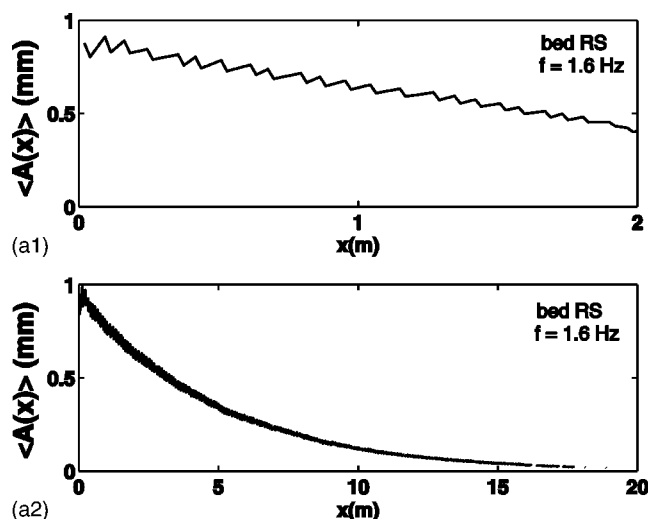


FIG. 7. The averaged variation of the amplitude of wave elevation along the wave tank for the bed RS from Fig. 6 with $f = 1.6$ Hz. To show the behavior near the transmission site, the results are plotted in two length scales: (a1) up to 2 m and (a2) up to 20 m.

within the ranges $[H_0 - \Delta H, H_0 + \Delta H]$ and $[L_0 - \Delta L, L_0 + \Delta L]$, respectively; here, $\Delta H = 1.2425$ cm and $\Delta L = 2$ cm. Four different frequencies have been measured and simulated.

The experimental and simulation results for a given random realization of the random beds are presented in Fig. 6. It is shown that the theoretical results match remarkably well the experimental results. It is shown that the waves do not decay monotonically along the random bottom (without averaging), due to the manifestation of resonant modes of the beds. The resonances are sensitive to the frequency variation. We also found that the occurrence of the resonances is sensitive to the random configuration.

We have further computed the averaged variation of the wave amplitude along the random bed for a sufficiently large number of random configurations. We found that though smeared out a little by the averaging, the resonance feature remains for spatial points near the transmission and tends to diminish for large traveling paths. And the averaged amplitude decays exponentially with increasing traveling distances. As an example, in Fig. 7 we illustrate these by the results of the bed RS case with $f = 1.6$ Hz. The results in Fig. 7 also indicate that the exponential decay rate, associated with the localization length, may not be accurately obtained from measurements done on insufficiently long samples, as the fluctuation can be quite significant for small sample sizes.

IV. SUMMARY

In summary, we have considered the propagation of water surface waves over topographical bottoms. A transfer method has been developed to compute the wave field along the propagating path, the transmission, and reflection coefficients. The localization effects due to disordered bottom structures are also considered. The theory has been applied to analyze the existing experimental results. Some agreements and discrepancies are discovered and discussed. It is pointed out that more detailed experiments may be helpful in not only identifying the peculiar localization phenomenon, but in helping improve theories for water-wave propagation over rough bottoms.

ACKNOWLEDGMENT

This work received support from the National Science Council (Grant No. NSC-92-2611-M008-002).

-
- [1] M. S. Longuet-Higgins, *J. Fluid Mech.* **1**, 163 (1956).
 [2] E. F. Bartholomeuz, *Proc. Cambridge Philos. Soc.* **54**, 106 (1958).
 [3] J. W. Miles, *J. Fluid Mech.* **28**, 755 (1967).
 [4] D. H. Peregrine, *Adv. Appl. Mech.* **16**, 9 (1979).
 [5] R. E. Meyer, *Adv. Appl. Mech.* **19**, 53 (1979).
 [6] H. Kagemoto and D. K.-P. Yue, *J. Fluid Mech.* **166**, 189 (1986).
 [7] M. Belzons, E. Guazzelli, and O. Parodi, *J. Fluid Mech.* **186**, 539 (1988).
 [8] P. Devillard, F. Dunlop, and B. Souillard, *J. Fluid Mech.* **186**, 521 (1988).
 [9] C. M. Linton and D. V. Evans, *J. Fluid Mech.* **215**, 549 (1990).
 [10] J. N. Newman, *J. Fluid Mech.* **23**, 399 (1965).
 [11] A. Nachbin and G. C. Papanicolaou, *J. Fluid Mech.* **241**, 311 (1992).
 [12] J. H. Pihl, C.-C. Mei, and M. J. Hancock, *Phys. Rev. E* **66**, 016611 (2002); G. L. Gratalop and C.-C. Mei, *ibid.* **68**, 026314 (2003).
 [13] H. Lamb, *Hydrodynamics* (Dover, New York, 1932).
 [14] C.-C. Mei, *The Applied Dynamics of Ocean Surface Waves* (World Scientific, Singapore, 1989).
 [15] M. W. Dingemans, *Water Wave Propagation over Uneven Bottoms* (World Scientific, Singapore, 1997).
 [16] P. W. Anderson, *Phys. Rev.* **109**, 1492 (1958).
 [17] P. Sheng, *Introduction to Wave Scattering, Localization, and Mesoscopic Phenomena* (Academic Press, New York, 1995).
 [18] E. Guazzelli, E. Guyon, and B. Souillard, *J. Phys. (France) Lett.* **44**, L-837 (1983).
 [19] P. Devillard, F. Dunlop, and B. Souillard, *J. Fluid Mech.* **186**, 521 (1988).
 [20] M. Torres, J. P. Adrados, and F. R. Montero de Espinosa, *Nature (London)* **398**, 114 (1999).
 [21] M. Torres *et al.*, *Phys. Rev. E* **63**, 011204 (2000).
 [22] L.-S. Chen and Z. Ye, *Phys. Rev. E* **70**, 036312 (2004); e-print cond-mat/0312288.
 [23] Z. Ye, *Phys. Rev. E* **67**, 036623 (2003).